Supplementary Information (SI) for New Journal of Chemistry.

Wide potential window (1.3V) supercapacitive study of high entropy alloy and green carbon composite electrode with its application towards aqueous symmetric device

Gobinda Chandra Mohanty[1]*, Anu Verma[2]

[1]School of Nanoscience and Technology Indian Institute of Technology, Kharagpur, India

[2]School of Environmental Science and Engineering, Indian Institute of Technology, Kharagpur, India

*Corresponding authors.

E-mail address:

gobinda2020@kgpian.iitkgp.ac.in

Synthesis of green carbon:

The green carbon is prepared by pyrolysis technique of Rice straw agricultural waste. At first rice straw collected and cleaned by tap water followed by DI-water and dried. Then the RS-straw was cut into small pieces 1 to 2 mm size. Then the rice straw used in the for pyrolysis in absence of oxygen at 600 ℃ for 1 h to get the pyrolyzed material. This obtained material is further processed through ball milling as well as probe sonication to obtained green carbon.

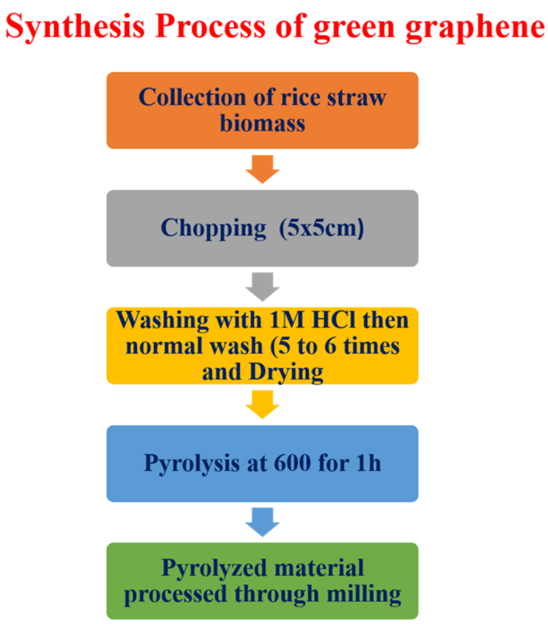

Figure S1: Schematic of synthesis of RS-biochar (green carbon) by pyrolysis technique.

3. Results and discussion

3.1. XRD

The XRD pattern of green carbon is shown the **Fig. S2(a)**. The angle of 2θ ranges from 20 to 30 with few intense peaks refers to graphene carbon structure with few Silica rich entity[1]. This XRD behaviour matched with graphene-silica rich green carbon. The previous is also backing same pattern[2, 3].

3.2. FTIR

Additionally, using the FT-IR spectrum, it has been possible to determine whether surface functional groups are present in green carbon. According to **Fig. S2 (b)**, the peak values are observed at 3443 cm^{-1}, 1639 cm^{-1}, 1049 cm^{-1}, 784 cm^{-1}, and 463 cm^{-1}. According to[4] the peaks at 3443 cm^{-1} and 1634 cm^{-1} are ascribed to the aromatic C=C bonds and the -OH stretching vibration, respectively. According to [5]a prominent peak seen at 1050 cm^{-1} is associated with asymmetric stretching (Si-O-Si), whereas 780 cm^{-1} is caused by symmetric vibration (Si-O-Si).

In addition, a band detected at 463 cm^{-1} could be attributed to the bending vibration of the Si-O-Si bond Older studies provide strong backing for these observations.

3.3. Raman studies

In order to investigate how graphene-based structures formed in the prepared sample, the Raman spectrum of the sample was also examined. The Raman spectrum displays two bands, as illustrated in **Fig. S2(c)**. According to[6], 1344 cm^{-1} and 1582 cm^{-1} bands, respectively), these are the D and G bands. Accordingly the sp^2 carbon structure is responsible for the G-band, which is a feature of graphitic substances (first order scattering of E_{2g} phonon). The presence of defects, such as A_{1g} symmetry and sp^3 disordered carbon, is what is responsible for the D-band, on the other hand. Indicating the presence of a multi-layer graphene structure, the relative intensity ratio of the Raman bands (I_D/I_G) is determined to be 1.

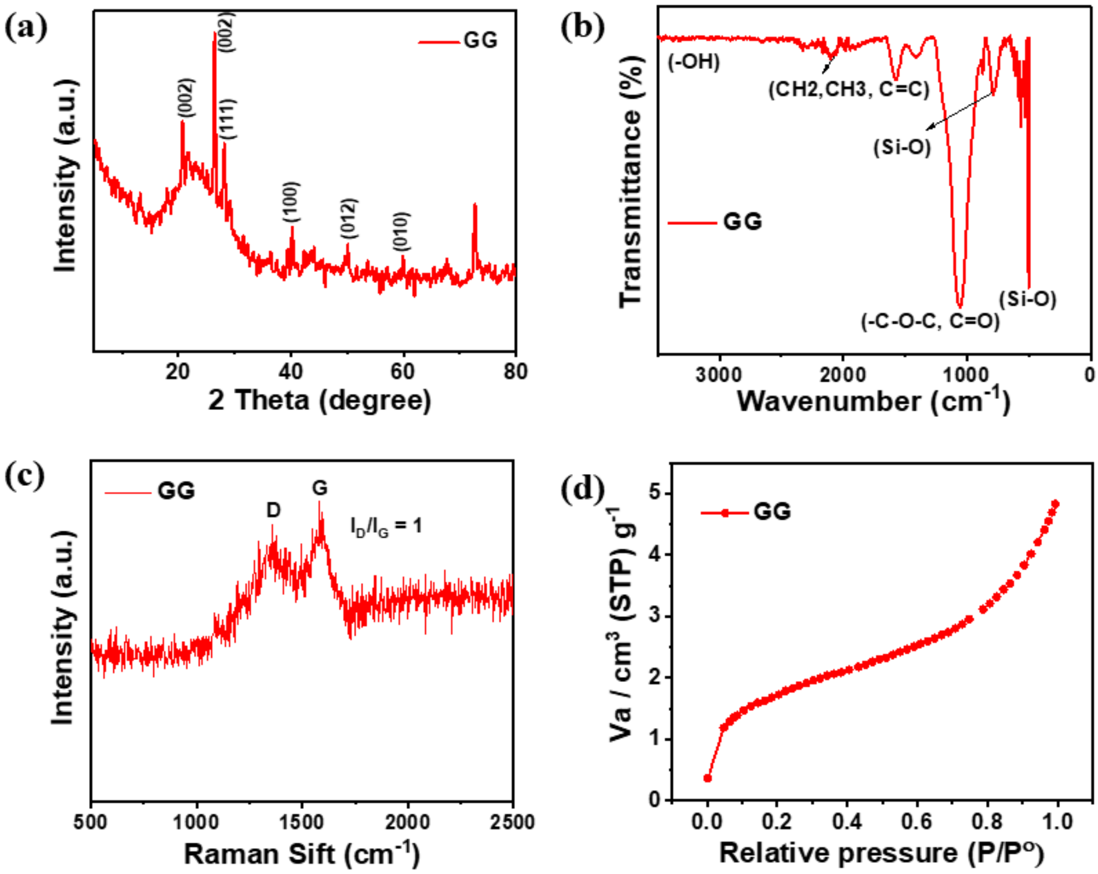

Fig. S2: (a) XRD (b) (FTIR) (c) Raman, and (d) BET plot

3.4. BET

Through N_2 physical adsorption measurements carried out at 77 K, an analysis of the porous structure of GGs has been investigated, and the results are displayed in **Fig. S2 (d)**. According to[7,8] this graph can be categorised as a type-II curve. It is seen that the graphs exhibit increased adsorption up to a relative pressure (p/p°) of 0.8 with a relatively low N_2 sorption profile. This might be attributable to the capillary condensation that occurs within the GGs mesoporous channels. However, between relative pressures of 0.8 and 1.0, a relatively higher N_2 sorption characteristic could be observed, which suggests that GGs may have a microporous structure[9]. BET specific surface area and mean pore diameter were reported to be 7.3 m^2/g and 4.6 nm, respectively. Furthermore, 7.4 cm^3/g of total pore volume was discovered.

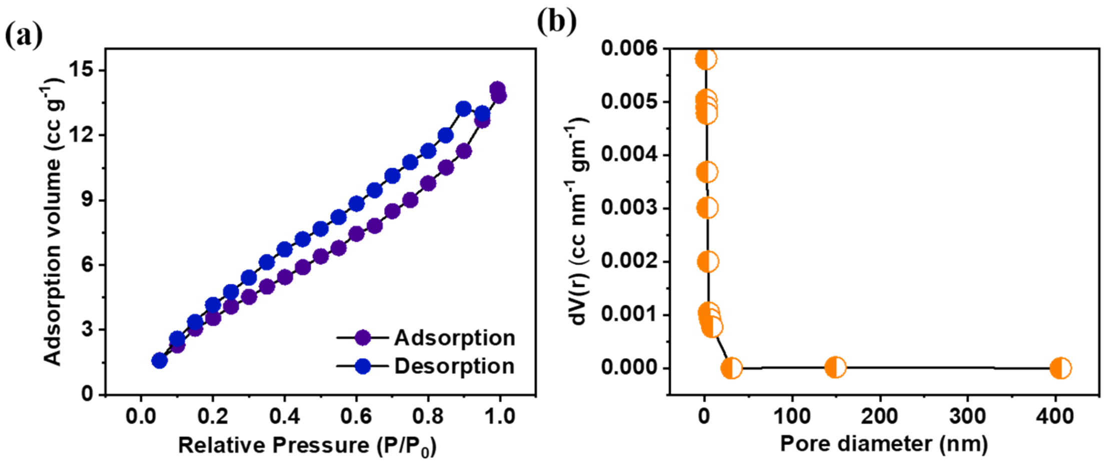

Figure S2: BET adsorption, desorption, and pore size distribution.

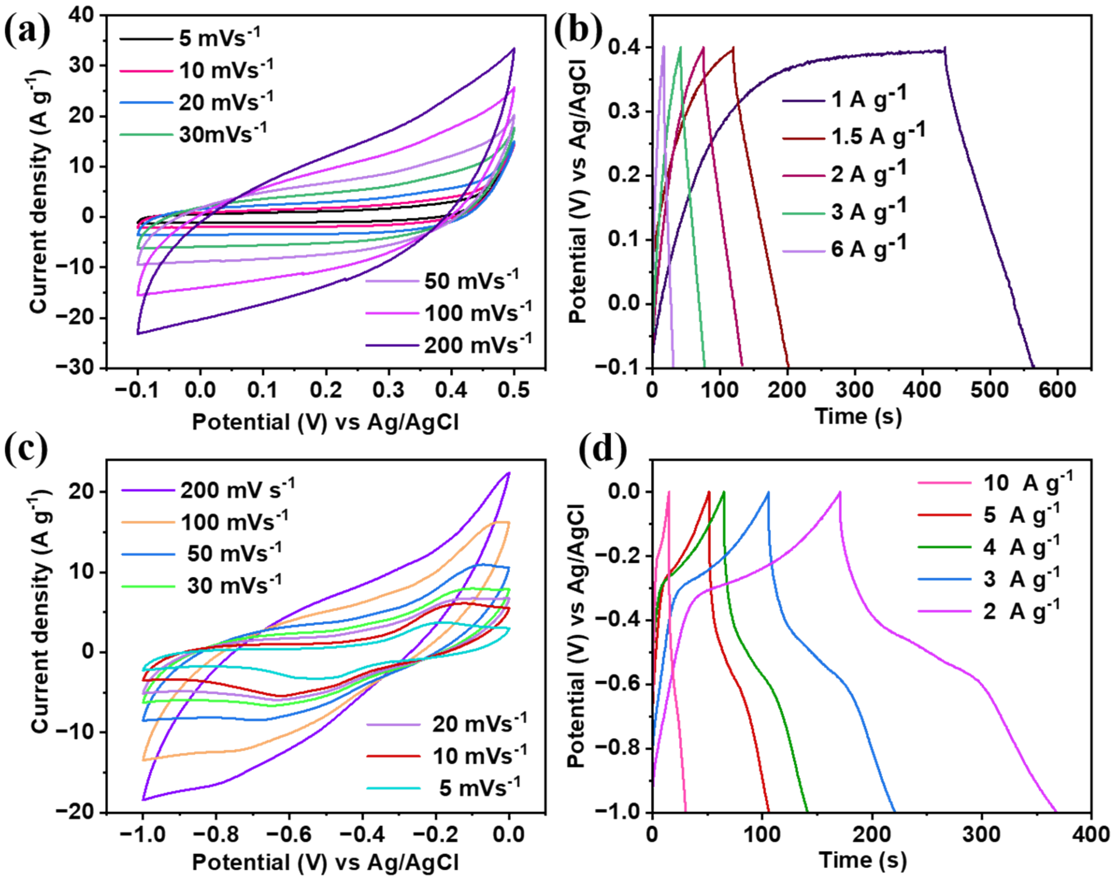

Figure S3: *(a, b) CV and GCD curves of FeCoNiCrMn HEA electrode, (c, d) CV and gcd curves of green carbon electrode.*

References:

(1) Autthawong, T.; Namsar, O.; Yu, A.; Sarakonsri, T. Cost-Effective Production of SiO2/C and Si/C Composites Derived from Rice Husk for Advanced Lithium-Ion Battery Anodes. *J. Mater. Sci. Mater. Electron.* **2020**, *31* (12), 9126–9132. https://doi.org/10.1007/s10854-020-03442-3.

(2) Sharma, S. K.; Sharma, G.; Sharma, A.; Bhardwaj, K.; Preeti, K.; Singh, K.; Kumar, A.; Pal, V. K.; Choi, E. H.; Singh, S. P.; Kaushik, N. K. Synthesis of Silica and Carbon-Based Nanomaterials from Rice Husk Ash by Ambient Fiery and Furnace Sweltering Using a Chemical Method. *Appl. Surf. Sci. Adv.* **2022**, *8*, 100225. https://doi.org/10.1016/j.apsadv.2022.100225.

(3) Tian, H.; Zhang, C.; Wang, Q.; Miao, J.; Zhang, Y.; Li, X.; Guo, Y.; Wang, M.; Chen, Y. SiO2 Aerogel @ Carbon Nanotube Anchored on Graphene Sheet as Anode Material for Lithium Ion Battery. *J. Mater. Sci. Mater. Electron.* **2021**, *32* (9), 11478–11488. https://doi.org/10.1007/s10854-021-05661-8.

(4) Haeri, S. Z.; Ramezanzadeh, B.; Asghari, M. A Novel Fabrication of a High Performance SiO2-Graphene Oxide (GO) Nanohybrids: Characterization of Thermal Properties of Epoxy Nanocomposites Filled with SiO2-GO Nanohybrids. *J. Colloid Interface Sci.* **2017**, *493*, 111–122. https://doi.org/10.1016/j.jcis.2017.01.016.

(5) Narayanan, D. P.; Sankaran, S.; Narayanan, B. N. Novel Rice Husk Ash - Reduced Graphene Oxide Nanocomposite Catalysts for Solvent Free Biginelli Reaction with a Statistical Approach for the Optimization of Reaction Parameters. *Mater. Chem. Phys.* **2019**, *222*, 63–74. https://doi.org/10.1016/j.matchemphys.2018.09.078.

(6) Choudhary, R.; Koppala, S.; Swamiappan, S. Bioactivity Studies of Calcium Magnesium Silicate Prepared from Eggshell Waste by Sol–Gel Combustion Synthesis. *J. Asian Ceram. Soc.* **2015**, *3* (2), 173–177. https://doi.org/10.1016/j.jascer.2015.01.002.

(7) Oh, W.-C.; Nguyen, D. C. T.; Areerob, Y. Enhanced Photocatalytic H2-Production and Photocatalytic Degradation Activity of Cadmium Oxide–Graphene Nanocomposite Grown on Mesoporous Silica under Visible Light Irradiation. *J. Porous Mater.* **2020**, *27* (1), 151–163. https://doi.org/10.1007/s10934-019-00796-w.

(8) Zhu, L.; Nguyen, D. C. T.; Woo, J.-H.; Zhang, Q.; Cho, K. Y.; Oh, W.-C. An Eco-Friendly Synthesized Mesoporous-Silica Particle Combined with WSe2-Graphene-TiO2 by Self-

Assembled Method for Photocatalytic Dye Decomposition and Hydrogen Production. *Sci. Rep.* **2018**, *8* (1), 12759. https://doi.org/10.1038/s41598-018-31188-w.

(9) Wang, J.; Chen, T.; Xu, B.; Chen, Y. Fabrication and Characterization of Porous Core–Shell Graphene/SiO2 Nanocomposites for the Removal of Cationic Neutral Red Dye. *Appl. Sci.* **2020**, *10* (23), 8529. https://doi.org/10.3390/app10238529.